Cavitations Analysis on Impeller Blades of Thai-made Irrigation Pump by Computational Fluid Dynamic technique

Benya Kasantikul[1] and Santi Laksitanonta[2]

[1] Department of Mechanical Engineering, Faculty of Engineering,
Kasetsart University, Khampaengsaen Campus, Nakornphathom, Thailand 73140
[2] Department of Mechanical Engineering, Faculty of Engineering,
Kasetsart University, Bangkok, Thailand 10900

Abstract

This research aims to study the cavitations on impeller blades of Thai-made Irrigation Pump. The diameter of mixed - flow impeller is 234 mm, tests at 900 rpm. Computational Fluid Dynamic technique (CFD) is used to predict the behaviors of the internal flow, the causes of cavitations and the area of cavitations occurrence on impeller blade. The cavitations occurrence is explain in terms of head at the exit, Net Positive Suction Head (NPSH), total head pump, pressure distribution and rate of vaporization at the different NPSH. Volume of Fluid (VOF) is the cavitations model which used to analyze and the Stepanoff's design parameters is used for the flow and in pump and on impeller blades. Boundary condition of total pressure is reduced until the cavitations occur. The result from CFD analysis shows that the cavitations occur in low pressure area, which causes high speed. The cavitations area starts from leading edge along to the tip. When NPSH is reduced, the cavitations area moves from leading edge to the trailing edge. The NPSH curve is lowered when cavitations number is more than maximum chord of impeller.

Key words: Thai-made irrigation pump, Cavitations, CFD

1. Introduction

Nowadays, Thai-made irrigation pumps are greatly playing a role in agriculture, using these pumps in farm, vegetable garden, orchard, and aquaculture farms. Advantages of these pump is easy to use and move, low cost and small factories can construct them on their own. Thai-made irrigation pumps are suited for pumping water that lowers banks about 1-4 m at the area where it is installed. If water levels are lower than that level, it is not functional because the water is too low to pump. The knowledge and understanding of these flow phenomena is used for design the high performance pump. One important point that causes a problem in low performance pump system is cavitations. At the present, several factors are determined for avoiding cavitations but, in the working state, there are always cavitations that effect high flow passage, etc. Cavitation makes low performance on pumping system and corrosive impeller. The study at the working state of the pump can be examined. The inception cavitations and can be modified to avoid or prevent the cavitation, to obtain the best performance or find the best cavitations point. Several literatures used the computation fluid dynamic for flow simulation

and got a good visualization of flow phenomena in pumps. [3-4, 8]

This article focuses on the hydraulically detailed performance analysis, including the cavitation phenomena, of a mixed-flow pump for marine water jet propulsion. Thus, the present study has employed the well-established commercial computational fluid dynamics (CFD) codes [12, 13], whose predictive capabilities have already been validated in the open literature and a variety of industrial applications: unsteady flow computation in a centrifugal compressor [7],CFD application to internal flow analyses of a water jet pump [5], the design and performance analysis of a centrifugal blood pump [9], hydraulic performance analysis of axial-flow pump [10] and radial-inflow turbine [11].

Computational Fluid Dynamics (CFD) is a powerful tool which can be used in evaluating and predicting incipient cavitation because several cavitation models have been developed. In this paper, Volume of Fluid (VOF) model has been used to clarify occurrence of cavitation in a flow passage of a mixed-flow pump. A cavitation model has been implemented based on the use of the Rayleigh Plesset Equation to estimate the rate of vapor production. The aim of this paper is to present results obtained with ANSYS CFX predicting inception cavitation as well as generation of vapor bubble. From these results, formation of cavitation has been examined in term of the (impeller) discharge head. Three percent Net Positive Suction Head (NPSH), several variables fringe plot on blade to blade, view of inception cavitations are plotted to analyze generation of vapor bubble. Location of maximum formation cavitation rates on the blade surface while NPSH reduction can be presented in this study.

A mixed-flow pump model in numerical simulation is characterized by a high specific speed (NS 1.68). At operating design point develops flow rate of 40 kg/s, head of 2.98 m at speed of 900 rpm. The geometric blade impeller model is transferred to ANSYS CFX TurboGrid that is used to generate computational grid. Flow through a blade passage is simulating to predict incipient cavitation. The numerical simulation results have been discussed to explain generation of vapor bubbles and cavitations phenomenon that happen through the flow passage of mixed-flow pump

2. Impeller 3D Flow Simulation

A 3D CFD flow simulation was carried out on an isolated impeller from mixed-flow pump with 900 rpm. The main pump parameters and geometry are presented in Figure 1 and Table 1.

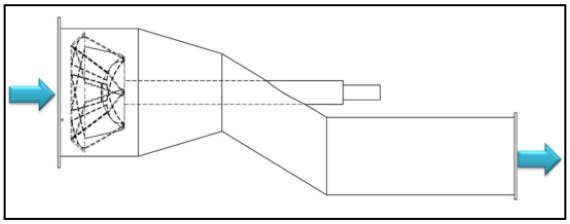

Figure 1: Visualization mixed-flow pumps [1].

Table 1: Geometrical parameters of the pump

mixed-flow pump[1,16]		
Parameter	Value	Description
Impeller		
R_0	117mm	Inlet flange radius
R_1	97.5mm	Mean impeller inlet radius
b_1	85.9mm	Inlet impeller width
β_1	59°	Inlet blade angle
θ_1	46°	Blade LE inclination angle
R_2	117mm	Mean impeller outlet radius
b_2	85mm	Outlet impeller width
β_2	68°	Outlet blade angle
Na	6	Blade number
e	3 mm	Blade thickness

The first task to accomplish on a numerical flow simulation is the definition of the geometry, followed by the grid generation. This step is maybe the most important step in this work. For the study of an isolated impeller, assuming an axisymmetric flow simplifies the domain to a single blade passage. The

simulation domain for the impeller mixed-flow pump is schematized in Figure 2. A structured grid was created using the ANSYS Turbogrid software.

2.1. Simulation parameters and boundary conditions

The general parameters and boundary conditions used for the 3D flow simulation of the impeller are summarized in Table 2. For all simulations, the boundary conditions are as follows.

(i) Inlet: total pressure applied in the rotation axis direction.

(ii) Outlet: imposed mass flow.

(iii) Periodic: two symmetry surfaces positioned in the middle of the blade passage.

(iv) Wall: general boundary condition by default. The simulation domain at the inlet and outlet sections was sufficiently extended to allow inlet recirculation and the elliptic influence of the flow.

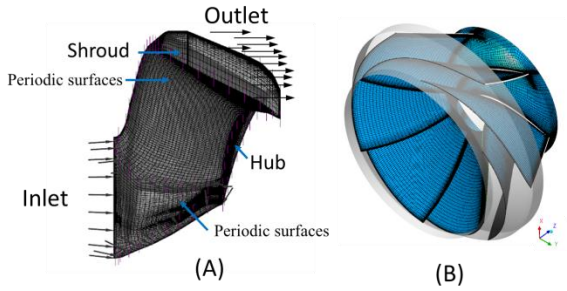

Figure 2: Impeller flow simulation domain and structured grid.

Table 2: Impeller simulation parameters

Parameters	ANSYS CFX
Flow simulation domain	Single impeller flow channel(periodic interface)
Grid	Structured
Inlet	Total pressure = 101325(Pa)
Outlet	Mass flow = variable (kg/s)
Turbulence model	*K - ω SST*[3,14]
Maximum residual convergence	10^{-4}(RSM)

2.2 Numerical methods

As a solver in this work ANSYS CFX is used. Code for solving equations for ideal gas used conservative forms of Navies Stokes Equations and k-ω SST turbulence model [3]. A part of the solver strategy used in ANSYS CFX is multigrid methods. The particular variant used in ANSYS CFX is based on conservation principles already implicit in the Finite Volume discretization and is called Additive Correction Multigrid. The linearized discrete algebraic equations that arise from most finite volume methods are sufficiently diagonally dominant to permit solution by simple relaxation methods.

2.3 Computational grid

The computational grid is generated with a multiblock grid generator based on transfinite interpolation. The computational grid is structured by 8 blocks with additional blocks at inlet and outlet of the computational domain. This grid has a relatively complex topology which gives it a high quality and avoids strongly skewed cells. The *O-mesh* around the blade allows for a good resolution of the leading and trailing edges. Total cells are 95000 hexahedral elements of structured grid used to model the computational domain. These 95000 cells are suitable to use for calculating by comparing the error value (grid dependent) with the number of cells, 1,100,000, 1,000,000, 950.00, 85,000, 700,000, and 600,000 cells. This amount of cells is appropriate for both of time spending and the error occurring in this calculation. The boundary layer of the blade is set to the value y + <2 [12].

2.4 Cavitations Model

VOF model is used to simulate flow with cavitation when local pressure decreases below vapor pressure. It is an effective model that is used in ANSYS CFX [3, 13].This model applied Rayleight-Plesset (RP) equation with the assumption that thermal and mechanical equilibrium exists between the phases. The RP equation provides the basis for the rate equation controlling vapor generation and construction

that can be solved by a volume of fluid (VOF) volume fraction with source term. The general advection-diffusion equation for the mass fraction of an individual component is given by [3, 13]

$$\frac{\partial}{\partial t}\left(\rho y_i\right)+\frac{\partial}{\partial x_j}\left(\rho u_j y_i\right)=\frac{\partial}{\partial x_j}\left(\Gamma_{i,eff}\frac{\partial y_i}{\partial x_j}\right)+S_{y,i} \quad \text{..... (1)}$$

The mass fraction conservation equation transformed to terms of a volume fraction equation as shown below.

$$\frac{\partial}{\partial t}\left(\rho_i \alpha_i\right)+\frac{\partial}{\partial x_j}\left(\rho_i u_j \alpha_i\right)=S_{\alpha,i} \quad \text{..... (2)}$$

To compute the rate of vapor generation and condensation, Rayleigh-Plesset has been used to derive source term. The rate of vaporization is given by

$$\dot{m}_V = N\rho_g \frac{dV_B}{dt} \quad \text{..... (3)}$$

and the rate of change of bubble volume is

$$\frac{dV_B}{dt} = \frac{d}{dt}\left(\frac{4}{3}\pi R_B^3\right) \quad \text{..... (4)}$$

The Rayleigh Plesset equation describing the growth of a gas bubble in liquid is given by

$$R_B\frac{d^2R_B}{dt^2}+\frac{3}{2}\left(\frac{dR_B}{dt}\right)^2+\frac{2\sigma}{R_B}=\frac{p_V-p}{\rho_1} \quad \text{..... (5)}$$

where RB represents the bubble diameter, pv is the pressure in the bubble, p is the pressure in the liquid surrounding the bubble and σ is the surface tension coefficient between the liquid and vapor.

3. Validation

In terms of validation, we tested the accuracy of the model by comparing calculated results with experimental results in simple shapes (2-D and 3-D hydrofoil) because they use less resource and save time in computing than the runner turbine, and many researches were done on how reliable hydrofoils are [17].

Since validation was proven, the simulation of cavitation flow on a bulb turbine was calculated in the next step. The application is a NACA0009 hydrofoil, truncated at 90% of the original chord length. It has the final dimensions of 100 mm of chord length. The 3D test section is modeled by a quasi 2D domain, with five rows of cells in spanwise direction for the numerical domain. The density of bubbles and the initial radius has been adjusted and fixed for all this study, n_0=1018 B/m^3, R_0=10^{-6}m. The computed domain (Fig. 4) is characterized by 9 blocks with C-type grid of (5×88000) mesh cells. The boundary conditions are set using a velocity inlet (C_{ref}=20 m/s) and a pressure at the outlet (the parameter which fixes the cavitation coefficient σ). Knowing that the cavity is located on the suction side of the hydrofoil, cavitations occur evidently. Figure 5-7 shows that the vapor volume fraction computed by the proposed cavitation model (with standard k-ε turbulence model) so we can conclude that it allow to design correctly the cavity shape. Figure 5-7 shows that the new model is on a good concordance with experimental results and it is able to evaluate correctly the evolution of the shape of cavity with decreasing σ.

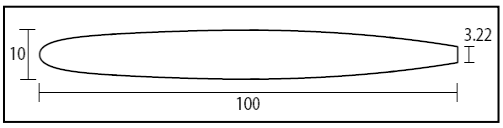

Figure 3: NACA0009 Hydrofoil

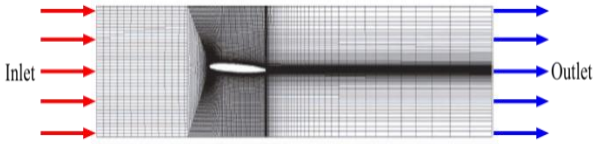

Figure 4: NACA0009 domain grid

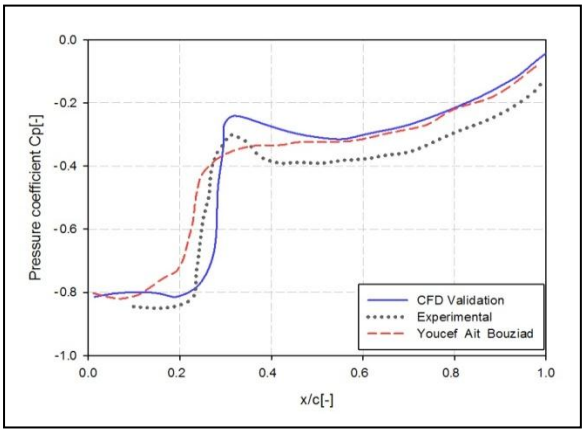

Figure 5: Numerical result and experimental (on NACA0009, i=2.5°, σ=0.85) [17]

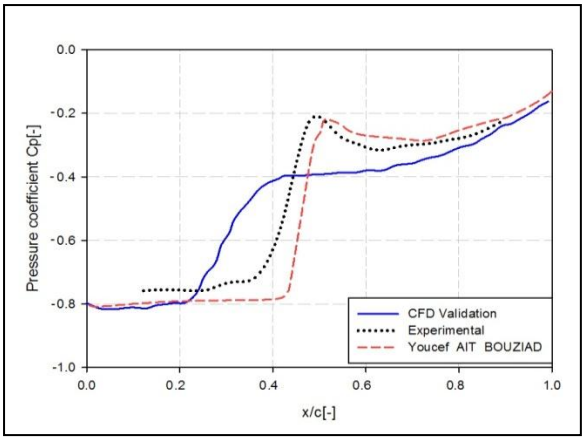

Figure 6: Numerical result and experimental (on NACA0009, i=2.5°, σ =0.75) [17]

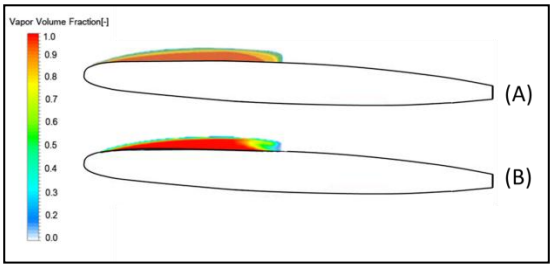

Figure 7: Pressure distribution and cavity shape on NACA0009 i=2.5°, σ =0.75,(A)[17] and (B) Validation

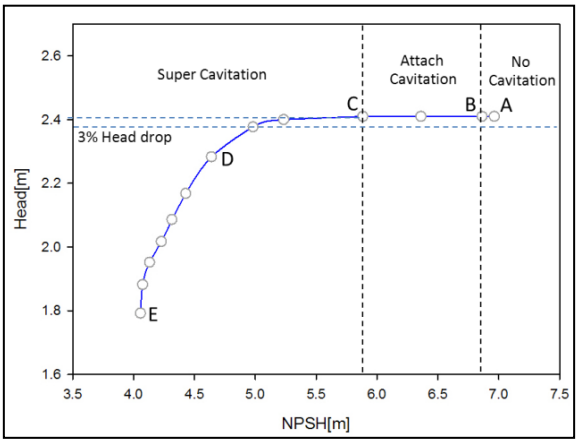

Figure 8: Head-NPSH curve at flow rate 40 kg/s and speed 900 rpm

The NPSH value is determined by the pressure difference between the inlet pressure and the minimum pressure in the flow passage and velocity head. [2, 6, 16]

$$NPSH = \frac{P_1 - P_{\min}}{\rho g} + \frac{C_1^2}{2g} \qquad \text{.....(5)}$$

Where $C_1 = \vec{V}_{circ} + \vec{V}_{merid}$

Figure 8: shows head drop curve as well as NPSH curve that computed by ANSYS CFX at design flow and rate speed. Volume of fluid model is selected as a cavitation model to compute rate of vapour bubble production. At inlet boundary total pressure is decreased to meet a status that cavitations formation is starting. NPSH 3% is the value at which the head below 3% of no cavitation head. From the head drop curve, predicted NPSH 3% can be evaluated about 4.72 m.

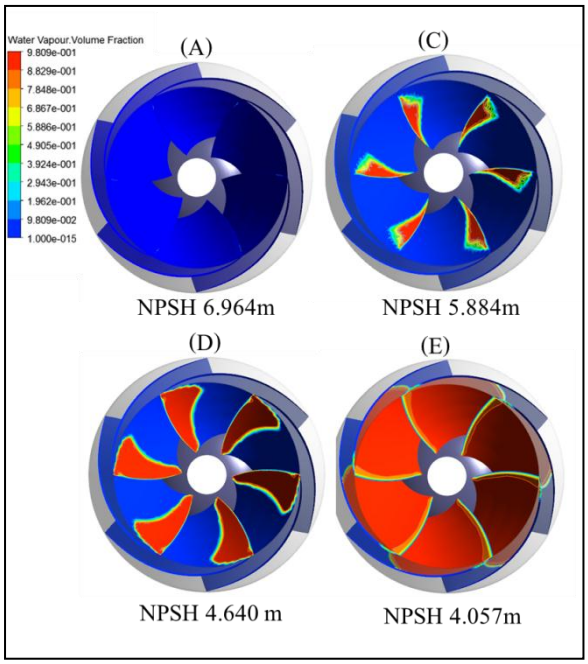

Figure 9: VAPOR Fringe Top view speed 900 rpm and flow rate 40 kg/s

Figure 9: shows cavity length with vapor fringe plot blade to blade view which corresponds to point A, C, D and E respectively in head drop curve (Figure 3). There is no

cavitation when NPSH = 6.964 m, attach cavitation when NPSH = 5.884m and super cavitation when NPSH = 4.640 m, NPSH = 4.057 as shown in figure 9. Therefore head drop curve in figure 8 can be divided according to cavity length on blade surface into three protions as no cavitation, attach cavitation and super cavitation [2]. No cavitations range from A to B in figure 8. In this portion rate of vapor production is approximately zero. Attach cavitation is range B to C that has cavity length on blade surface less than or equal chord length. Cavitation on suction surface is growing when decreasing NPSH. If cavity length grow up more than chord length, super cavitations occur as shown in figure 8-D. Super cavitation is range C to E in figure 8.

Location of Cavitation

To describe a change in the location of cavitation while NPSH value is decreased, the predicted bubble vaporization rate in the flow passage is shown.

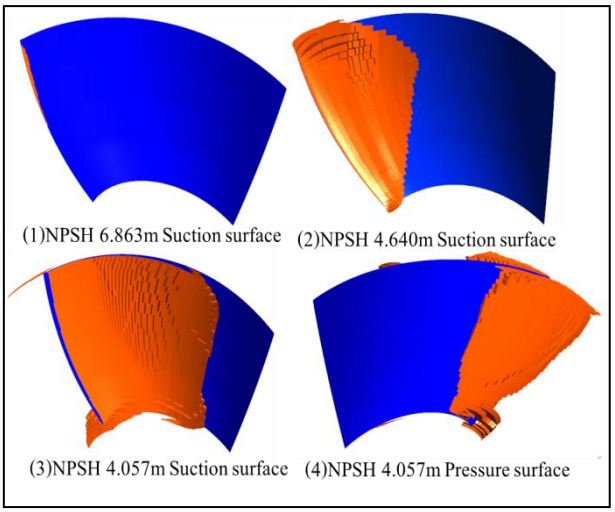

Figure 10: Fringe Plot showing cavitation on blade surface at speed 2400 rpm, flow rate 18 kg/s

Figure 10: shows VAPOR Fringe Plot with variation of NPSH. Figure 10-1 shows that the maximum evaporation rate occurred at the blade leading edge near the tip. Figure 10-2 shows that the location of maximum evaporation rate moves from the blade leading edge. Figure 10-3 shows that the maximum evaporation rates occur at the blade trailing edge near the tip. Figure 10-4 shows that cavitation occur on the pressure surface in case of super cavitation. Hence for NPSH value lower than NPSH value that inception cavitation form, the location of maximum evaporation rate move from the blade leading edge to the blade trailing edge along the stream line near the tip. Cavitation can be seen on pressure surface as shown in figure 10-4. If cavitation occurs on pressure surface, pump head corresponding point E on head drop curve figure 8 will decrease rapidly

Effect quantity of cavitation to head drop curve-NPSH

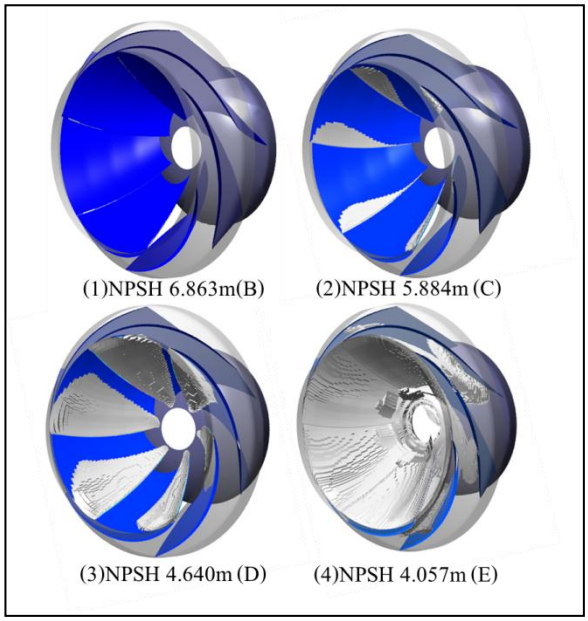

Figure 11: Shows quantity of cavitations that occurs on impeller at 900 rpm, 40 kg/s of mass flow rate.
(1) Inlet Total Pressure 7.0 $\times 10^4$ Pa
(2) Inlet Total Pressure 5.0 $\times 10^4$ Pa
(3) Inlet Total Pressure 3.4 $\times 10^4$ Pa
(4) Inlet Total Pressure 2.0 $\times 10^4$ Pa

Figure 11: shows the calculated cavitations quantity at 900 rpm, 40 mass flow rate and inlet total pressure 7.0 $\times 10^4$, 5.0 $\times 10^4$, 3.4 $\times 10^4$ and 2.0 $\times 10^4$ Pa. Inception cavitations formation start can be approximate when inlet total pressure value was about 7.0 $\times 10^4$ NPSH 6.863 m, vapor was combine and became the

cavitation that called “attach cavitation” as shown in figure 11-2. Head value was stable and when inlet total pressure was 3.4×10^4 Pa and NPSH was 4.640 m, generated the super cavitating that shown in figure 11-3. The cavity length was longer than impeller, head slightly decreased and immensely decreased when NPSH was 4.057 m as shown by (E) on NPSH head curve. The decreasing the head causes the vapor to be compressible, changing of the head at inception cavitations made stream line deviation. These causes affect the velocity, pressure and head was change.

5. Conclusion

From results, NPSH cure could separate cavity length on impellers to 3 groups, no cavitation, attach cavitation and super cavitation. No cavitation, head value was stable and cavitations did not occur but attach cavitations did occur during inception cavitations at NPSH 6.863 m, head value was stable when NPSH decreased. Super cavitation, head value decreased on the right angle changing character. NPSH 4.057 m, super cavitation was occurring. Inception cavitation made cavitation formation at suction surface on the leading edge area of the meeting tip and when NPSH decreased, inception cavitation position shifted from leading edge to trailing edge, considering stream wise direction. NPSH 4.057 m, inception cavitation was occurring at pressure surface that affected by cavitations on another impeller. The simulation of pump flowing by computation fluid dynamic can give a good understanding of flow phenomena in pumps. Nowadays, predictions of inception cavitation are complicate and not accurate, so by developing the generation and breaking up the vapor bubbles would create a more accurate result.

REFERENCES

[1] Kaewprakaisaengkul, C. (1996). Evaluation and improvement of Thai-made irrigation pumps. Thesis (Ph.D.)., Asian Institute of Technology.

[2] Brennen, C.E. (1994). Hydrodynamics of Pumps, Oxford University Press, London.

[3] Lifante, Conxita; Frank, Thomas (2008). Investigation of higher order pressure fluctuations and its influence on ship stern, taking into account cavitation at propeller blades, Final Report ANSYS / TR-08-04, Research Project No: 03SX202A

[4] H. Ding, F. C. Visser,Y. Jiang and M. Furmanczyk(2011).Demonstration and Validation of a 3D CFD Simulation Tool Predicting Pump Performance and Cavitation for Industrial Applications. *ASME J. Fluids Engineering* ,133:1.

[5] Oh, H. W., Yoon, E. S., Kim, K. S., and Ahn, J. W. (2003). A practical approach to the hydraulic design and performance analysis of a mixed-flow pump for marine waterjet propulsion. *Proc. Instn Mech. Engrs, Part A:J. Power and Energy*, 217(A6), 659–664.

[6] Balje, O. E. *Turbomachines: a guide to design, selection,and theory*, (1981) (JohnWiley, New York).

[7] Koumoutsos, A., Tourlidakis, A., and Elder, R. L.(2000). Computational studies of unsteady flows in a centrifugal compressor stage.*Proc. InstnMech.Engrs,Part A: J.Power and Energy*, 214(A6), 611–633.

[8] Hong Gao, W Lin, and Zhaohui Du. (2008). Numerical Flow and Performance Analysis of a Water-Jet Axial Flow Pump, Ocean Engineering, Vol.35, No.16, 1604-1614

[9] Oh, H.W., Yoon, E. S., Park, M. R., Sun, K., and Hwang,C. M.(2005). Hydrodynamic design and performance analysis of a centrifugal blood pump for cardiopulmonary circulation. *Proc. IMechE, Part A: J. Power and Energy*, 219(A7), 525–532.

[10] Oh, H. W., Yoon, E. S., and Park, S. J. (2006).Hydraulic performance analysis of an axial-flow main coolant pump for the system-integrated nuclear reactor. *Proc. IMechE,Part A: J. Power and Energy*, 220(A6), 635–640.

[11] Oh, H.W. and Yoon, E. S. (2007) Application of computational fluid dynamics to performance analysis of a Francis hydraulic

turbine. *Proc. IMechE, Part A: J. Power and Energy*, 221(A4), 583–590.

[12] *ANSYS TurboGrid12.1*, 2009 (ANSYS, Inc.).

[13] *ANSYS CFX 12.1* 2009 (ANSYS, Inc.).

[14] Menter, F. R., Kuntz, M., Langtry, R.,(2003) Ten Years of Industrial Experience with the SST Turbulence Model. In: Hanjali_c, K., Nagano, Y., Tummers, M. (Eds.), *Turbulence, Heat and Mass Transfer 4*, Begell House, pp. 625-632

[15] Bardina, J. E.,Huang,P. G., and Coakley,T. (1997). J. Turbulence modeling, validation, testing and development. NASA TM 110446.

[16] Stepanoff, A.J., (1975). Centrifugal and axial flow pumps Theory Design and Application, John Wiley, New York, pp.138-160.

[17] Youcef AIT, B. (2006). Physical modeling of leading edge cavitation : Computational methodologies and application to hydraulic machinery. Thesis (Ph.D.)., University of Paris.

NOMENCLATURE

$\dot{m}_v$ = total interphase mass transfer rate per unit volume

N = bubbles per unit volume

$NPSH_{3\%}$ = three percent head drop net positive suction head

P_1 = inlet static pressure

P_{t1} = inlet absolute total pressure

P_{t2} = outlet absolute total pressure

R_B = bubble radius

Sy,i = source term of component i

V_B = bubble volume

$\vec{V}_{circ}$ = circumferential plane velocity

$\vec{V}_{merid}$ = meridional velocity

y = mass fraction

α = volume fraction

n_0 = density of bubbles

R_0 = initial radius

C_{ref} = reference velocity

NPSH= Net Positive Suction Head

SST = shear stress transport